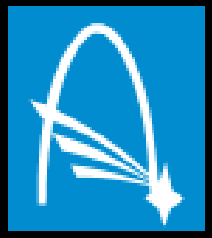

Thickness matters
in self-gravitating expanding shells

R. Wünsch, S. Ehlerová, J. E. Dale, V. Sidorin, J. Palouš, R. Smith, A. P. Whitworth, S. Walch

Outline:

1. **Observations of shells**
   → shells are everywhere

2. **Pressure Assisted Gravitational Instability**
   → AMR vs. SPH simulations vs. theory
   → Thickness matters

3. **Mass spectrum of fragments**
   → Oligarchic accretion leads to top-heavy clump mass function

Galactic bubble N107, Credit: Churchwell et al. (2006), Spitzer, GLIMPSE, IRAC, 8μm cont.

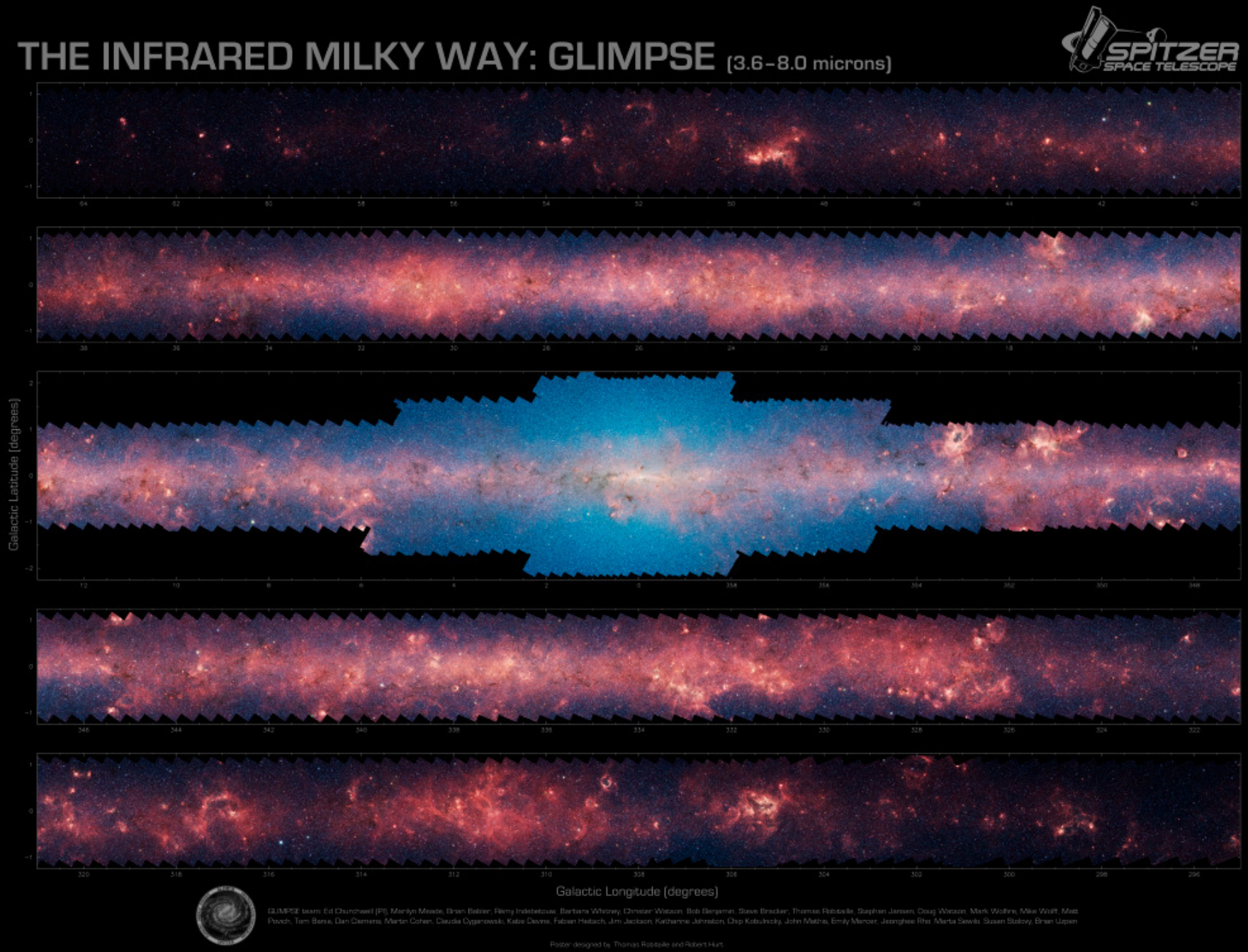
THE INFRARED MILKY WAY: GLIMPSE (3.6–8.0 microns)
SPITZER SPACE TELESCOPE
Galactic Latitude (degrees)
Galactic Longitude (degrees)
GLIMPSE team: Ed Churchwell (PI), Marilyn Meade, Brian Babler, Remy Indebetouw, Barbara Whitney, Christer Watson, Bob Benjamin, Steve Bracker, Thomas Robitaille, Stephen Jansen, Doug Watson, Mark Wolfire, Mike Wolff, Matt Povich, Tom Bania, Dan Clemens, Martin Cohen, Claudia Cyganowski, Kate Devine, Fabian Heitsch, Jim Jackson, Katherine Johnston, Chip Kobulnicky, John Mathis, Emily Mercer, Jeonghee Rho, Marta Sewilo, Susan Stolovy, Brian Uzpen
Poster designed by Thomas Robitaille and Robert Hurt

The bubbling galactic disk

(Churchwell et al., 2006)

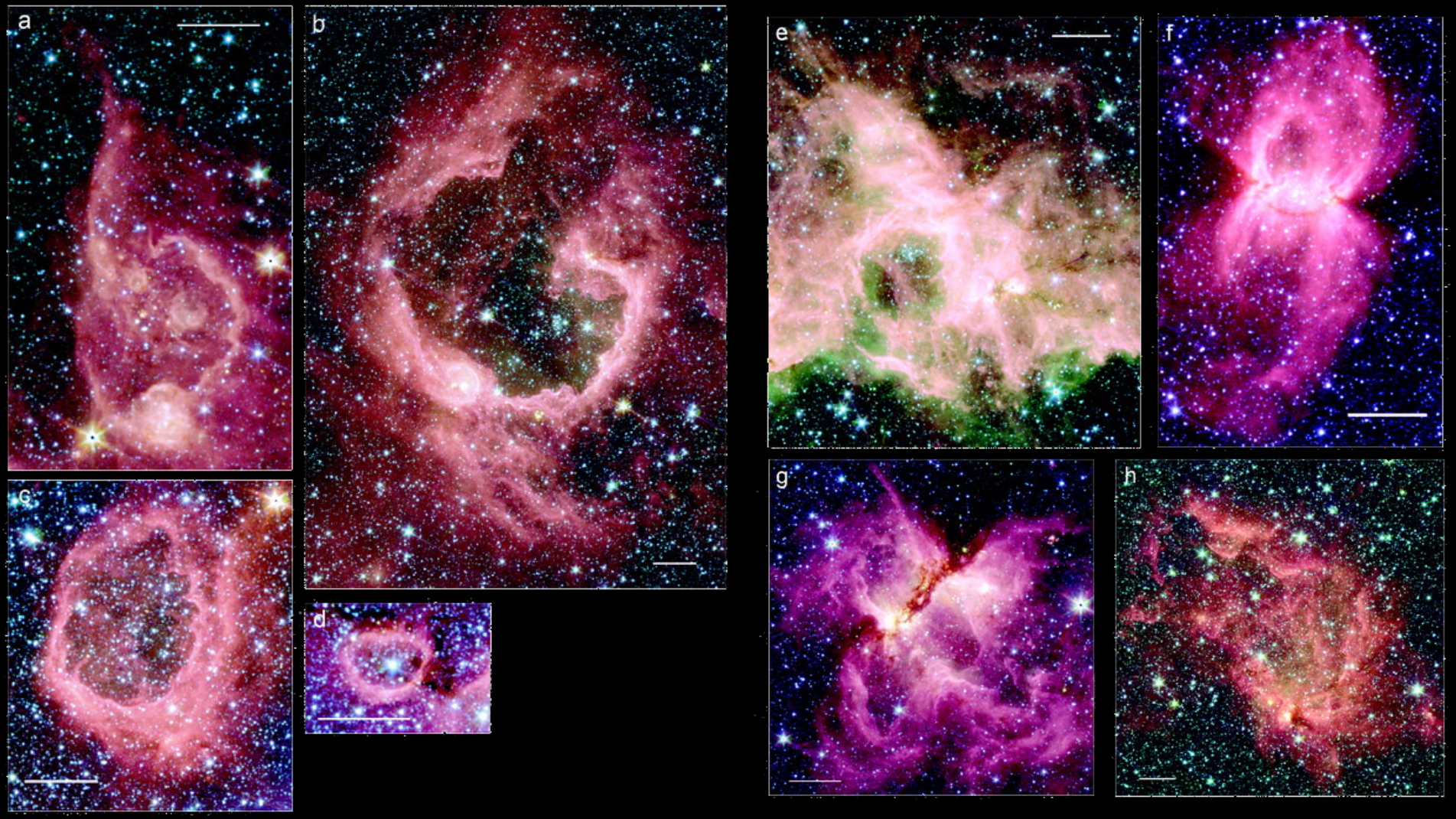

Spitzer bands: 4.5μm (blue), 5.8μm (green), 8μm (red)

Bubbles are everywhere

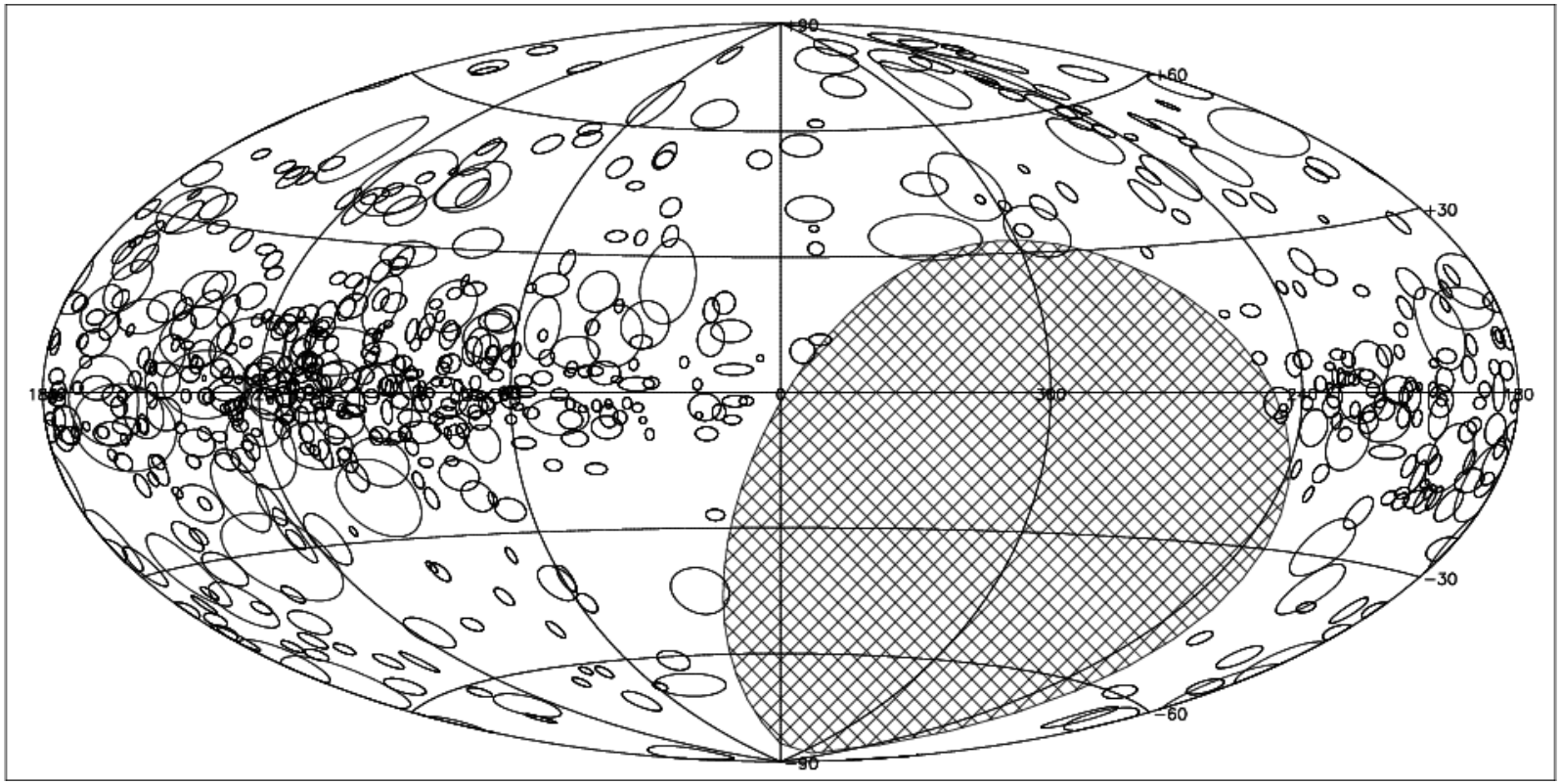

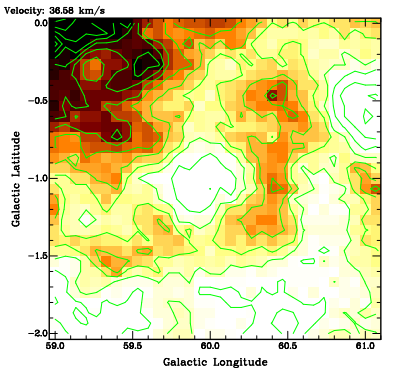

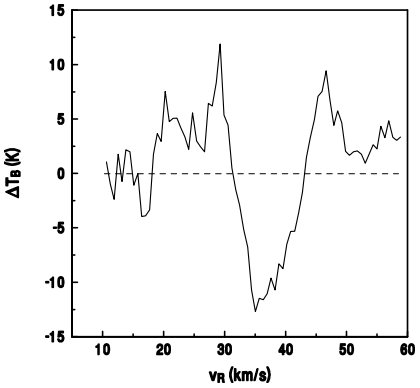

automatic search for HI shells in Leiden-Dwingeloo survey
→ statistical study of 300 HI shells in 2nd quadrant
(Ehlerová et al. 2005)

Bubble properties

- radii: $r \sim 10$ pc - 2 kpc
- expansion velocities: $v_{\rm exp} \sim 5 - 30$ km/s
- formation energy: $E \sim 10^{51} - 10^{53}$ erg
- observed in many wavelengths: HI (IGALFA, . . .), IR (Spitzer/GLIMPSE,. . .), Hα (WHAM), mm (CO lines), radio cont., X-rays
- observed in MW and many nearby galaxies (LMC, SMC, M31, M33, IC10 . . .)
- origin: OB stars (fossils of expanding HII regions), encounters with HVC or dwarf galaxy, GRB, turbulence and instabilities in ISM
- implications: source of information about ISM, Disk-halo connection, **Triggered star formation (Collect and Collapse)**

Collect and collapse

(Elmegreen & Lada, 1977)

HII region Sh 104 (Deharveng et al., 2003)

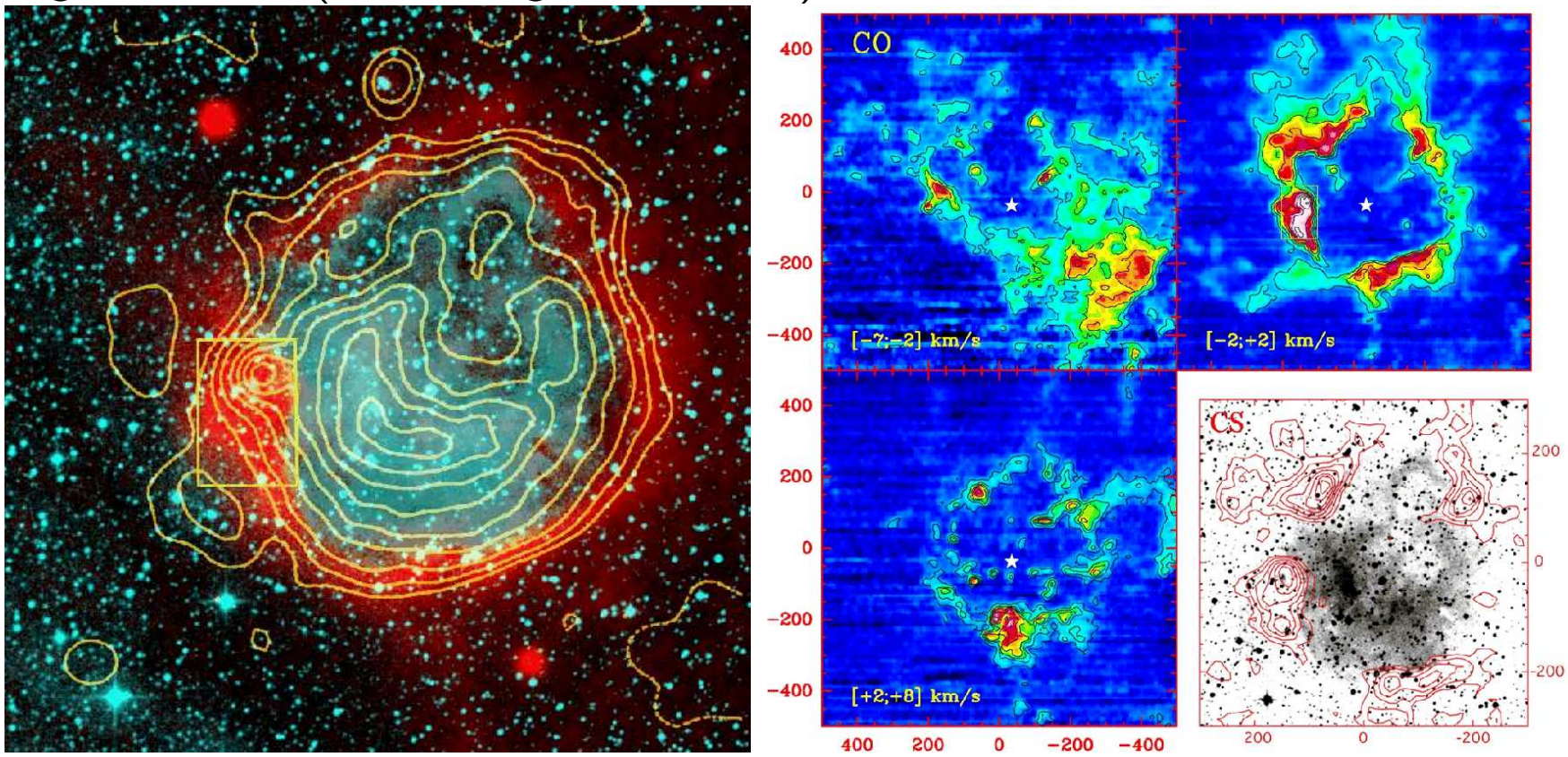

Left: contours (thermal radio continuum 1.46 GHz), red (mid-IR emmision - PAHs), turquoise (Hα - ionized gas)
Right: CO molecular line at different velocities

Multiwavelength study of N107

(Sidorin, 2008)

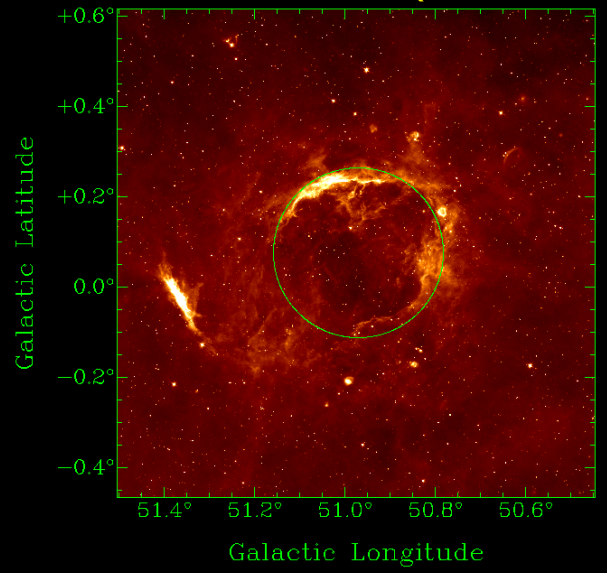

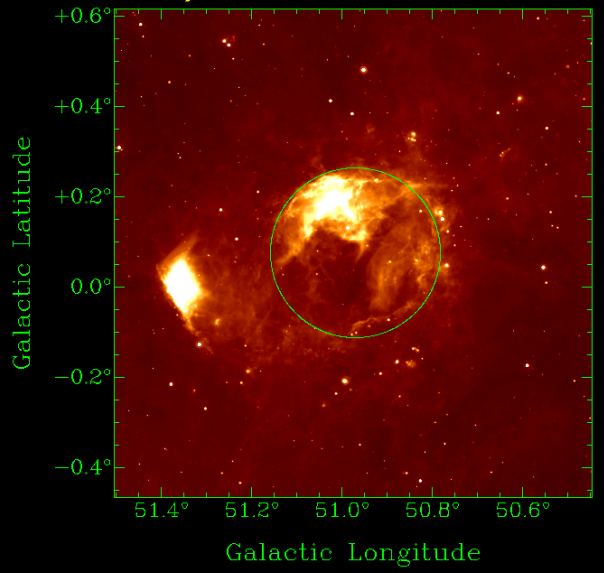

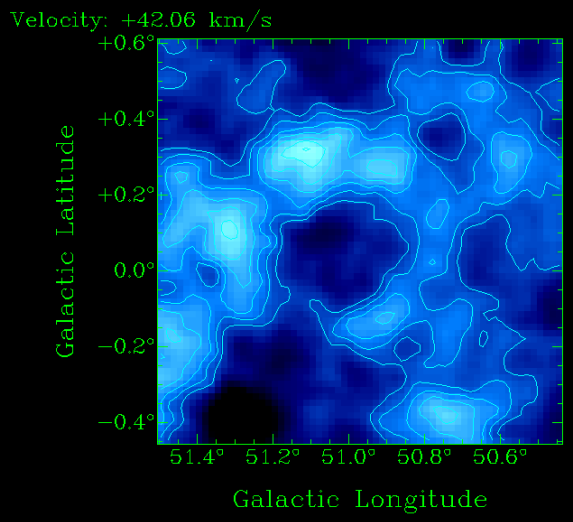

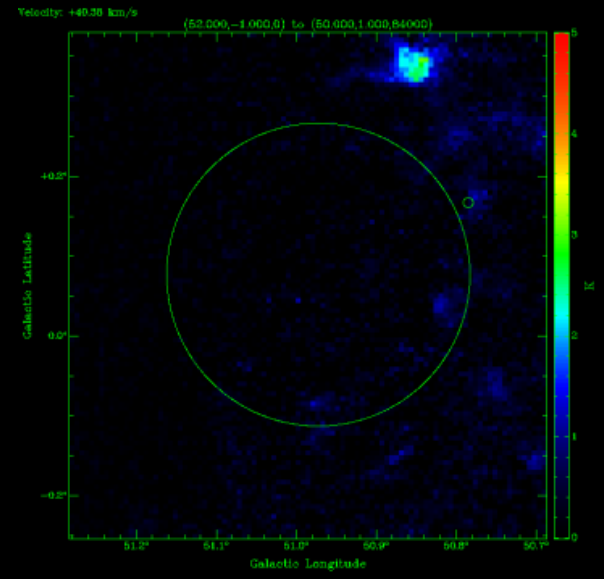

Expanding shell instabilities

- gravitational instability (long time-scale)
- Rayleigh-Taylor instability

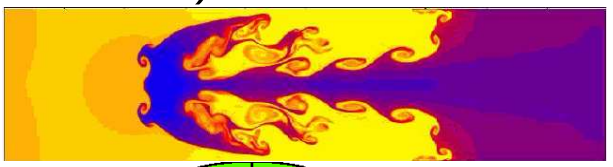

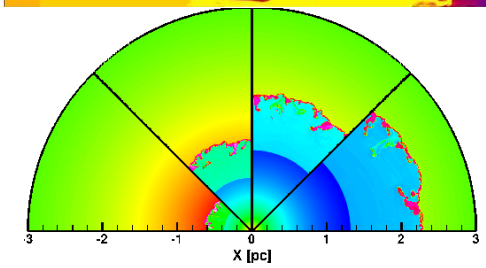

- Vishniac instability
  (Vishniac, 1983; 1994)
- magnetic field:
  Parker inst. (Parker 1966)

  Wardle inst. (Wardle, 1990)

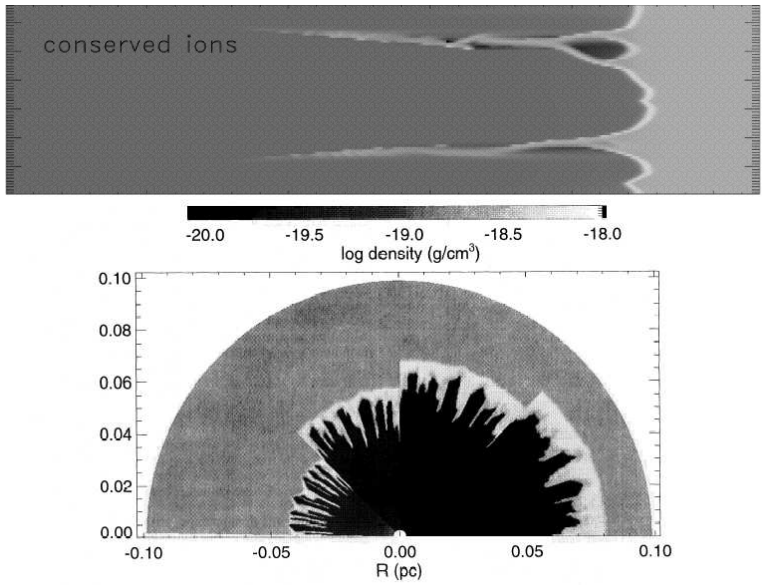

FIG. 6.—Evolution of the I-S front instability for a case with constant density (model UC32). The cooling cutoff is 10^3 K, and the time step is 5×10^3 yr. The ambient medium has $n_0 = 10^3$ cm^{-3} and $T_0 = 100$ K, and the stellar flux is $F_* = 10^{48}$ s^{-1}. This model is equivalent to the very early stages of model S32, shown in Fig. 8.

- ionized shell instability
  (Garcia-Segura & Franco, 1996)

Simulation setup

- extremely simplified model to avoid instabilities other than the gravitational one
  (RT, Vishniac)
- ballistic shell (in a free fall) embedded in a rarefied medium

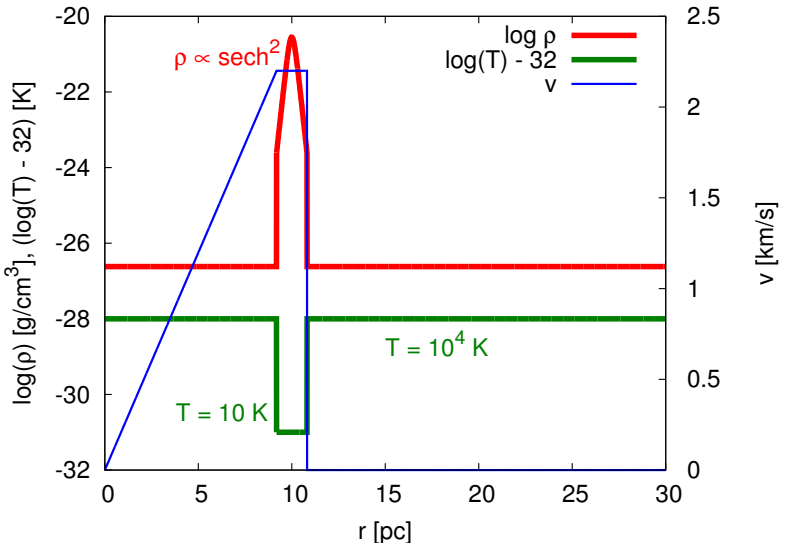

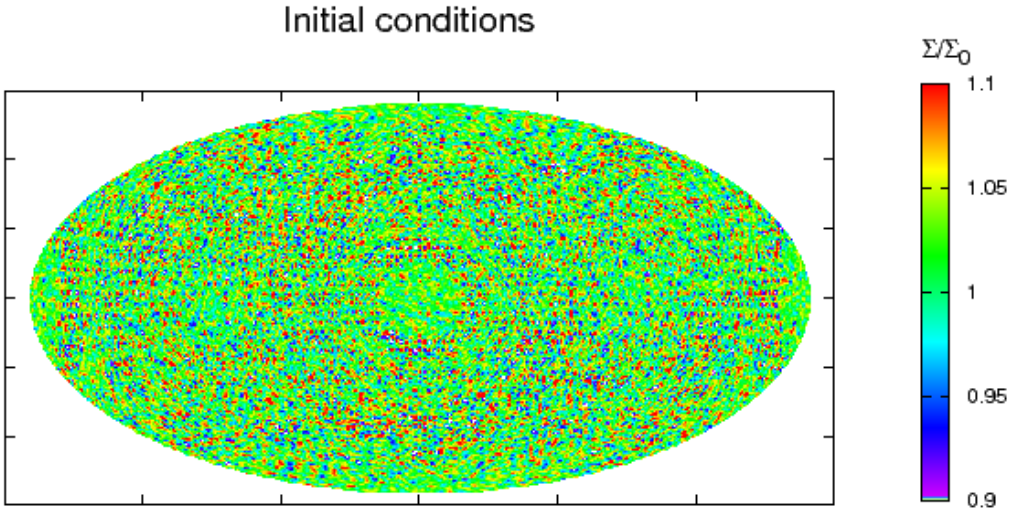

$M_{\rm shell} = 2 \times 10^4$ M$_\odot$
$T_{\rm shell} = 10$ K
$R_{\rm shell,0} = 10$ pc
$V_{\rm shell,0} = 2.2$ km s^{-1}
$R_{\rm shell,max} = 23$ pc
$P_{\rm ext} = 10^{-17}, 10^{-13}$
or 5×10^{-13} dyne cm^{-2}

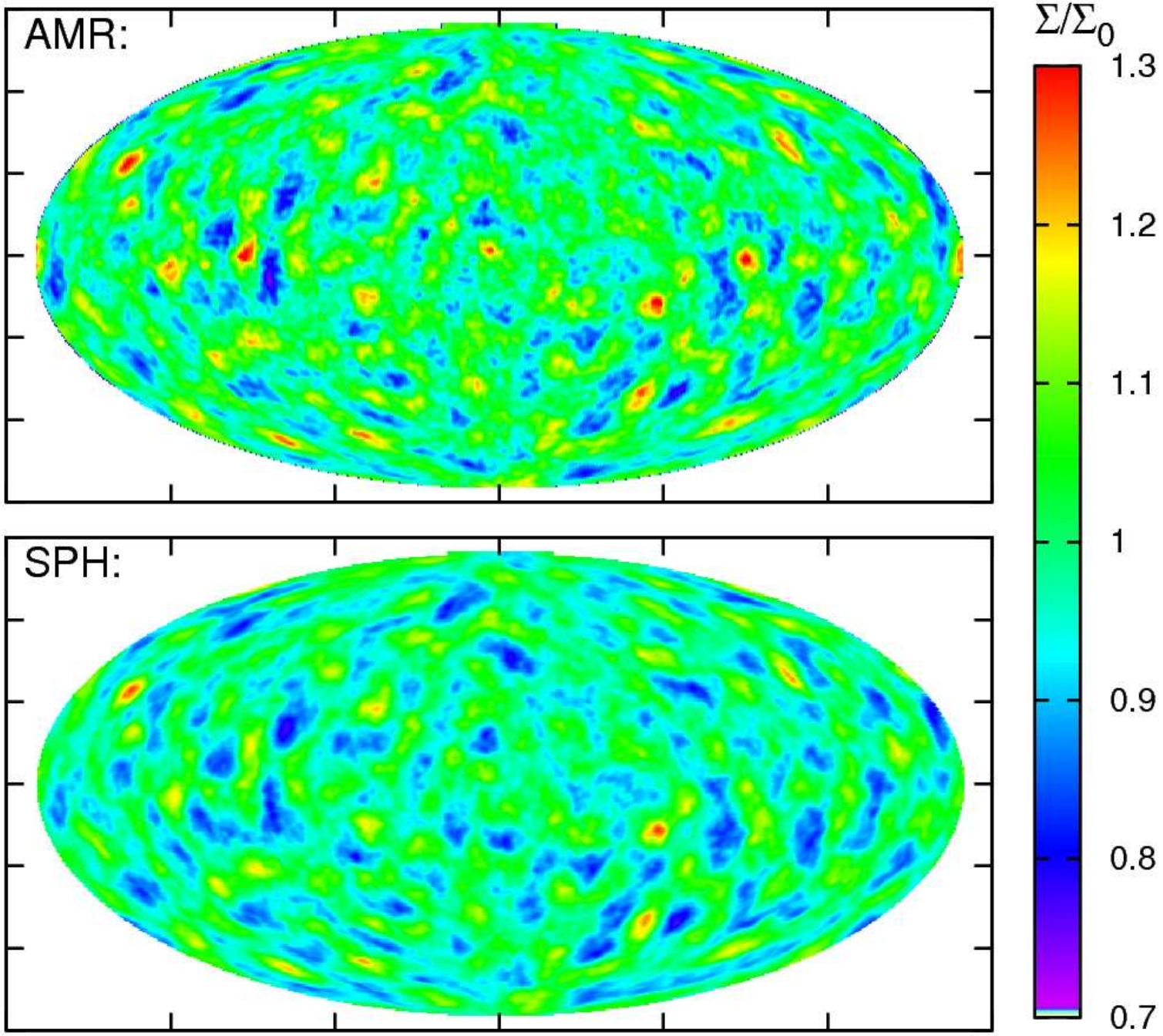
AMR:
SPH:
Σ/Σ_0
1.3
1.2
1.1
1
0.9
0.8
0.7

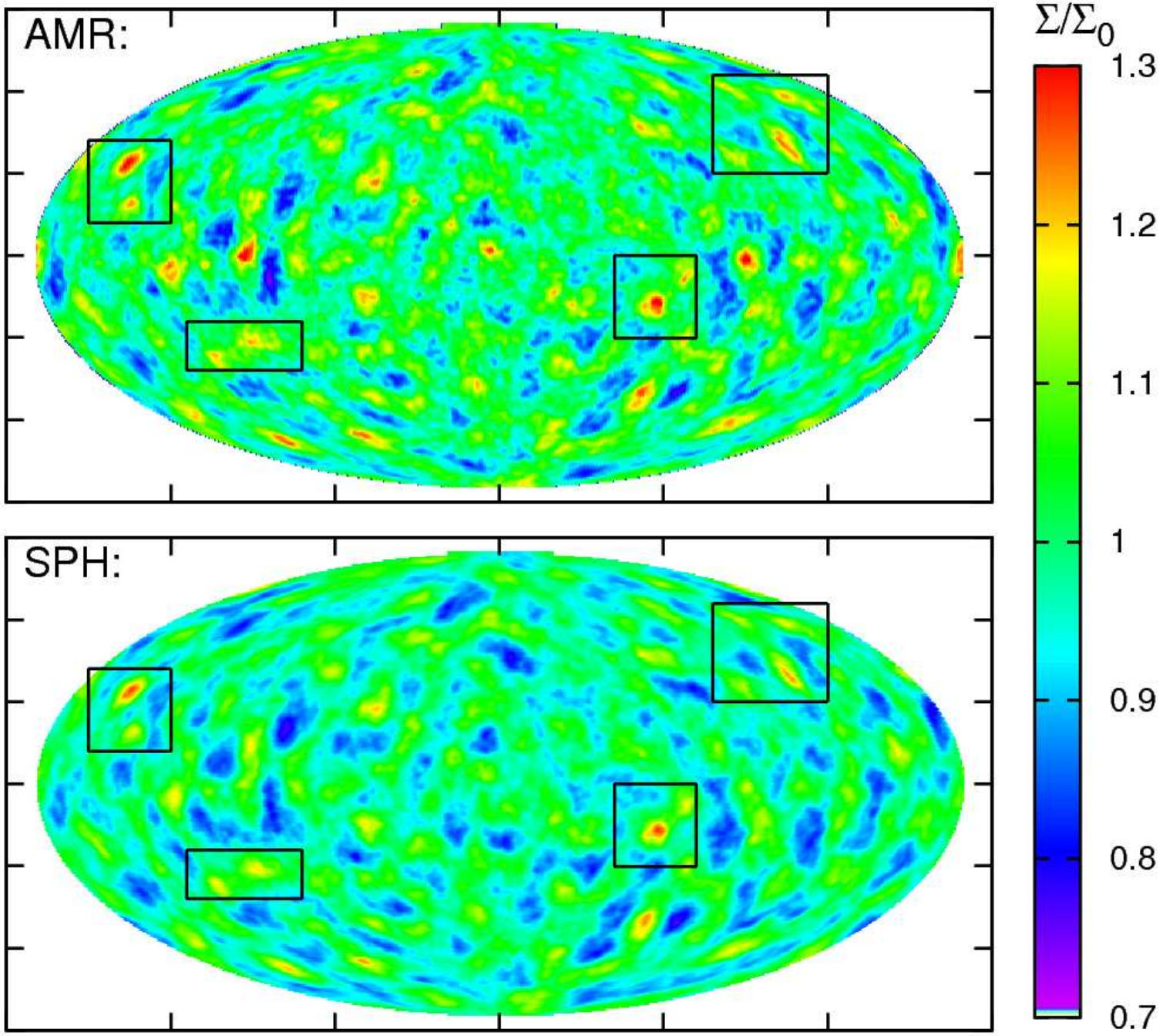
AMR:
SPH:
Σ/Σ_0
1.3
1.2
1.1
1
0.9
0.8
0.7

Find six differences!

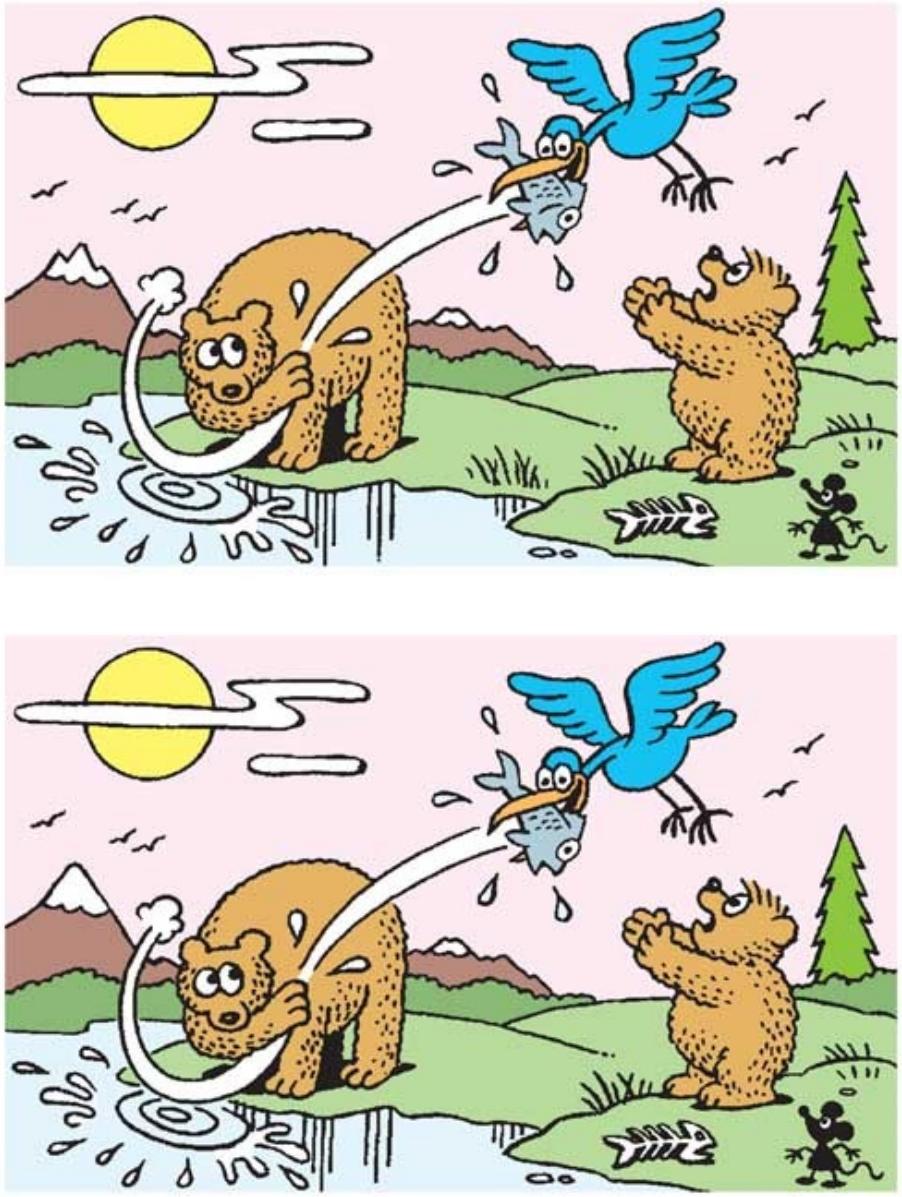

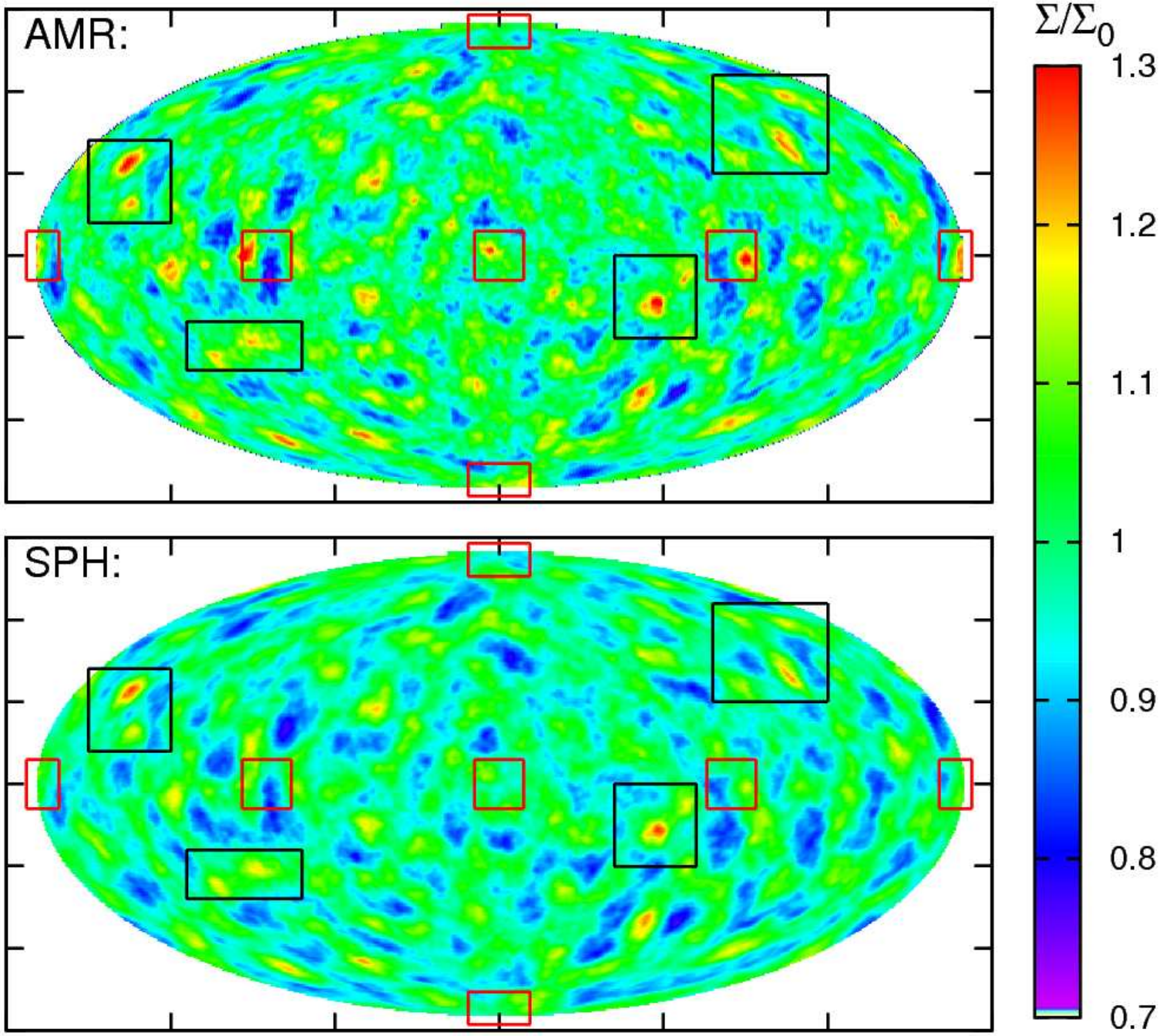
AMR:
SPH:
Σ/Σ_0
1.3
1.2
1.1
1
0.9
0.8
0.7

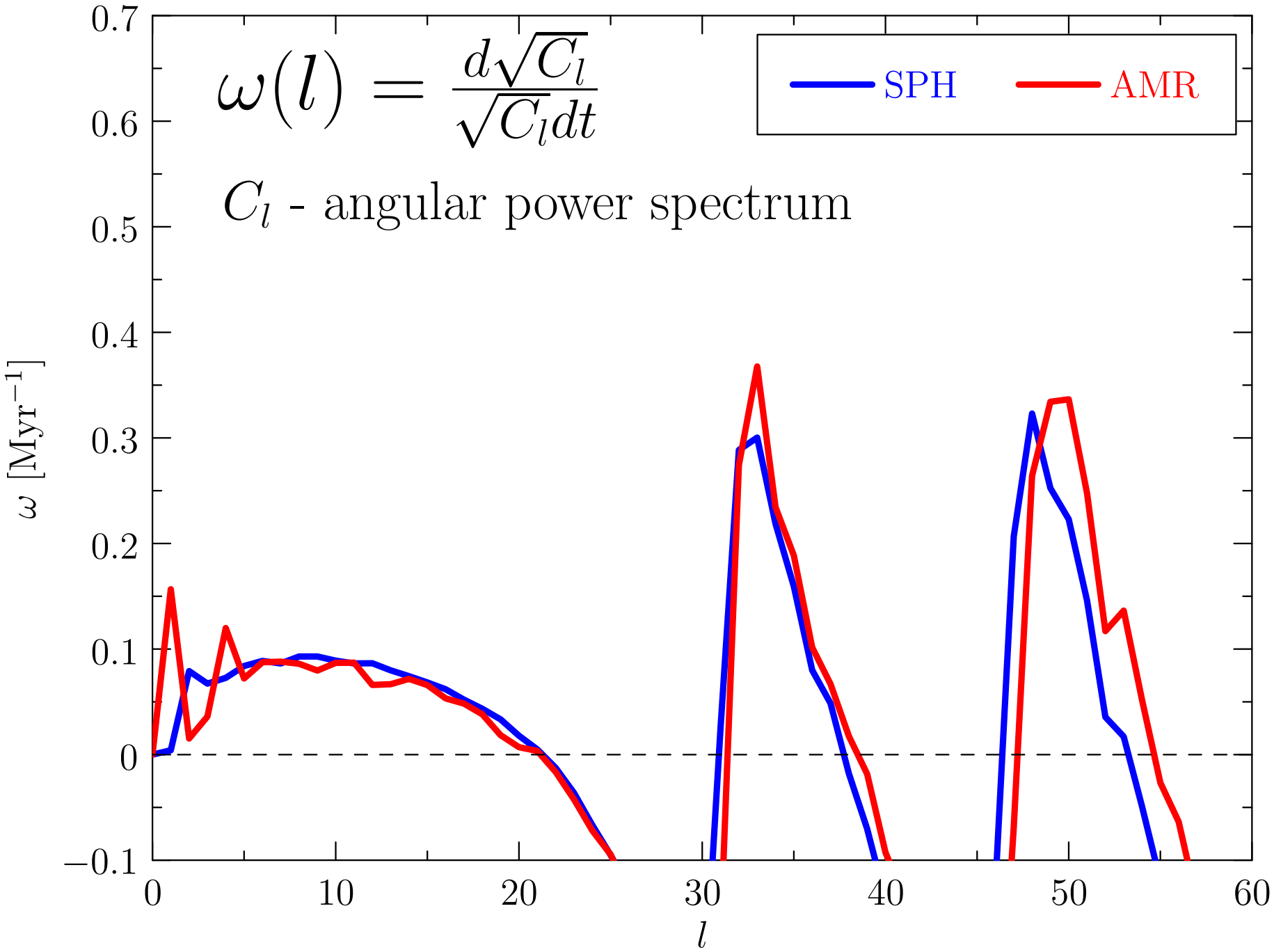
$\omega(l) = \frac{d\sqrt{C_l}}{\sqrt{C_l}dt}$
C_l - angular power spectrum
SPH
AMR
ω [Myr^{-1}]
l
0.7
0.6
0.5
0.4
0.3
0.2
0.1
0
−0.1
0
10
20
30
40
50
60

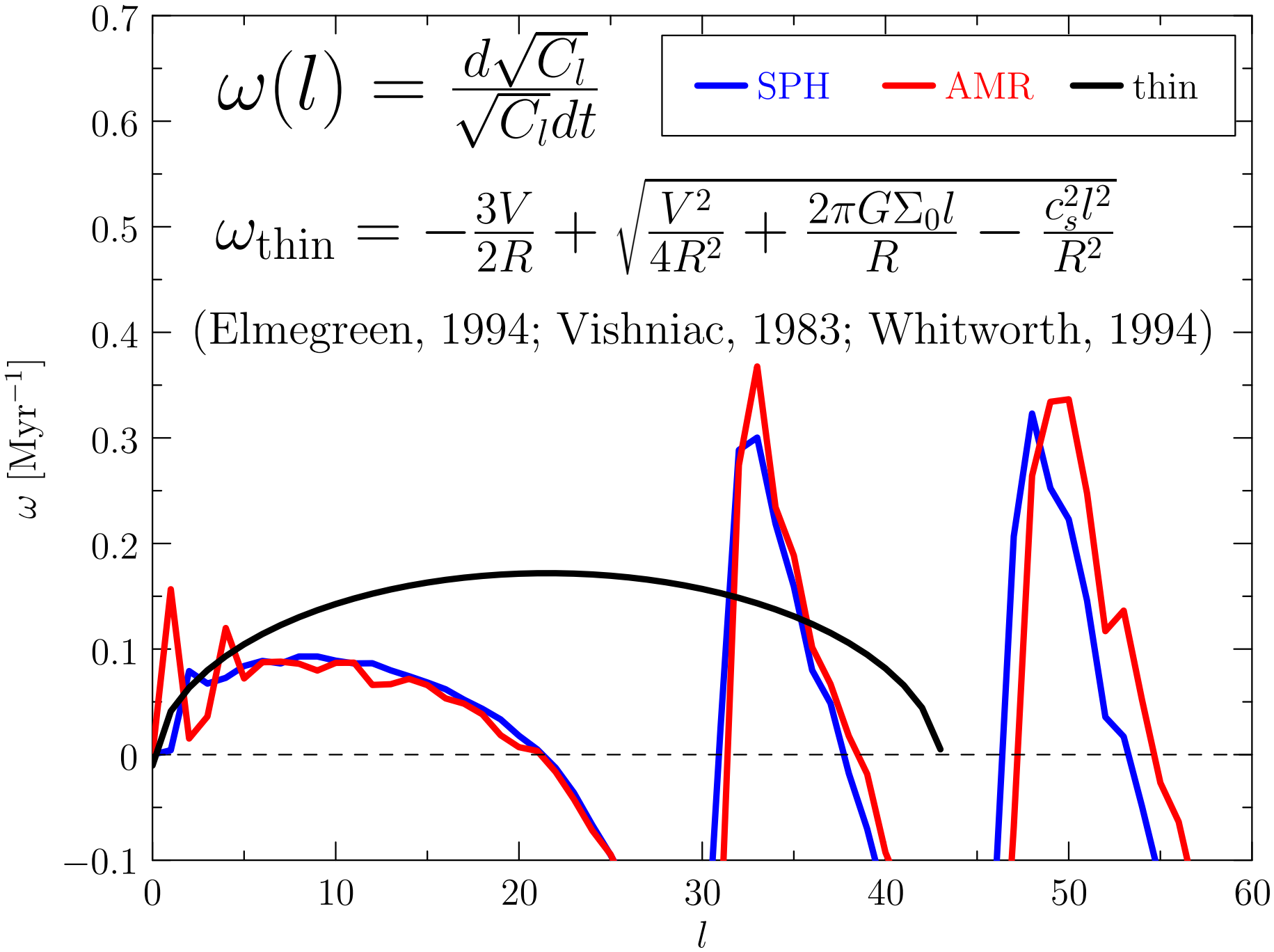
$\omega(l) = \frac{d\sqrt{C_l}}{\sqrt{C_l}dt}$
SPH
AMR
thin
$\omega_{\rm thin} = -\frac{3V}{2R} + \sqrt{\frac{V^2}{4R^2} + \frac{2\pi G\Sigma_0 l}{R} - \frac{c_s^2 l^2}{R^2}}$
(Elmegreen, 1994; Vishniac, 1983; Whitworth, 1994)
ω [Myr^{-1}]
l
0.7
0.6
0.5
0.4
0.3
0.2
0.1
0
−0.1
0
10
20
30
40
50
60

Gravitational instability of thin shell

(Vishniac, 1983; Whitworh et al. 1994; Elmegreen, 1994)

pressure gravity stretching accretion

$$\Sigma_0 R\frac{\partial \mathbf{\Omega}}{\partial t} = -c_s^2\nabla\Sigma_1 + \Sigma_0\nabla\Phi_1 - \Sigma_0\mathbf{\Omega}V - 3\Sigma_0\mathbf{\Omega}V$$

$$\frac{\partial\Sigma_1}{\partial t} = -\Sigma_0 R\nabla_{\mathrm{T}}\cdot\mathbf{\Omega} - 2\Sigma_1\frac{V}{R}$$

stretching

$$\nabla^2\Phi_1 = 4\pi G\Sigma_1\delta(r-R)$$

$\rightarrow$ linearization, perturbations inserted
mode with dimensionless wavenumber $l = kR$ studied:

$$\omega_{\mathrm{thin}}(l) = -\frac{3V}{R} + \sqrt{\frac{V^2}{R^2} + \frac{2\pi G\Sigma_0 l}{R} - \frac{c_s^2 l^2}{R^2}}$$

High pressure ambient medium

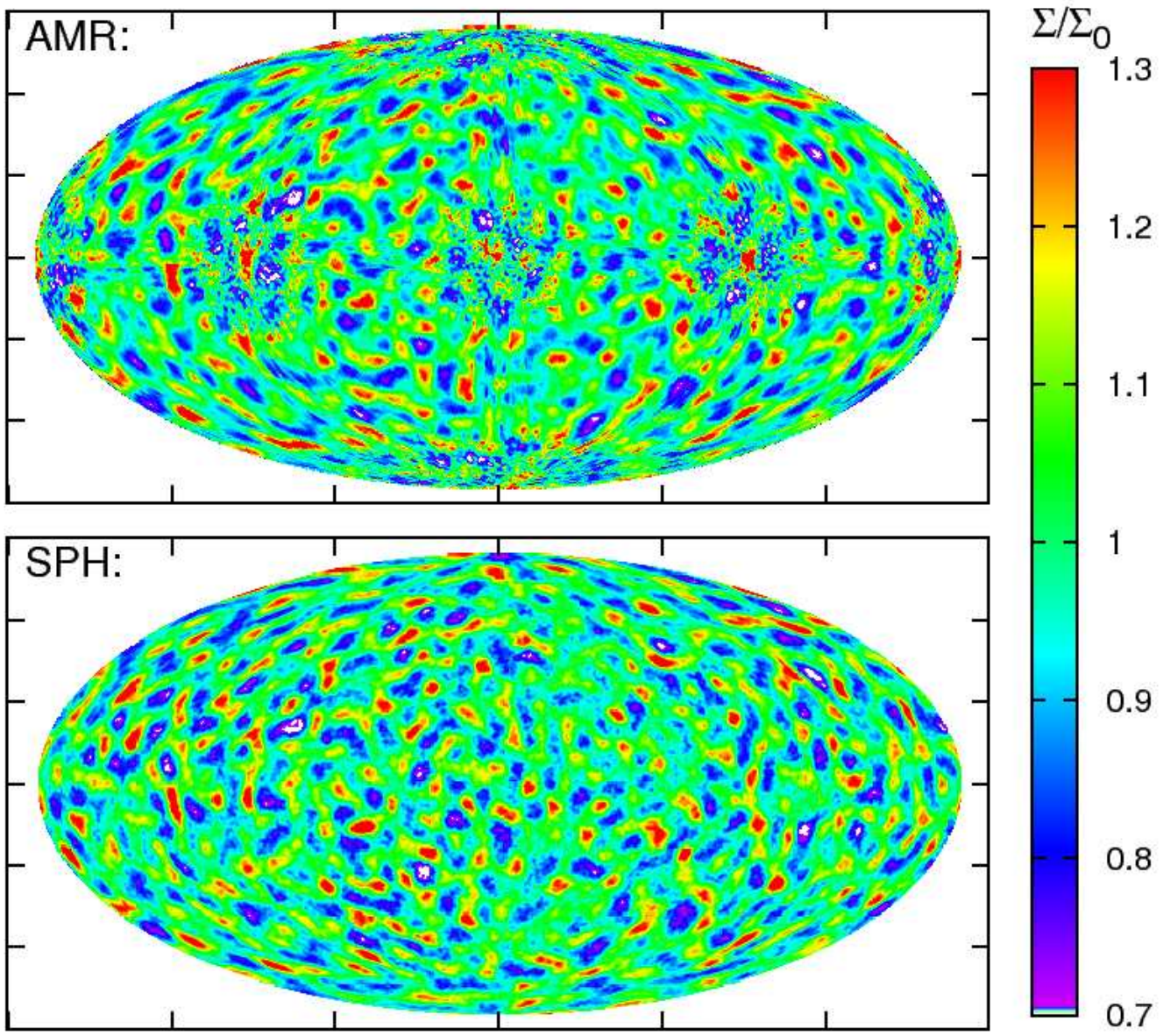

High pressure ambient medium

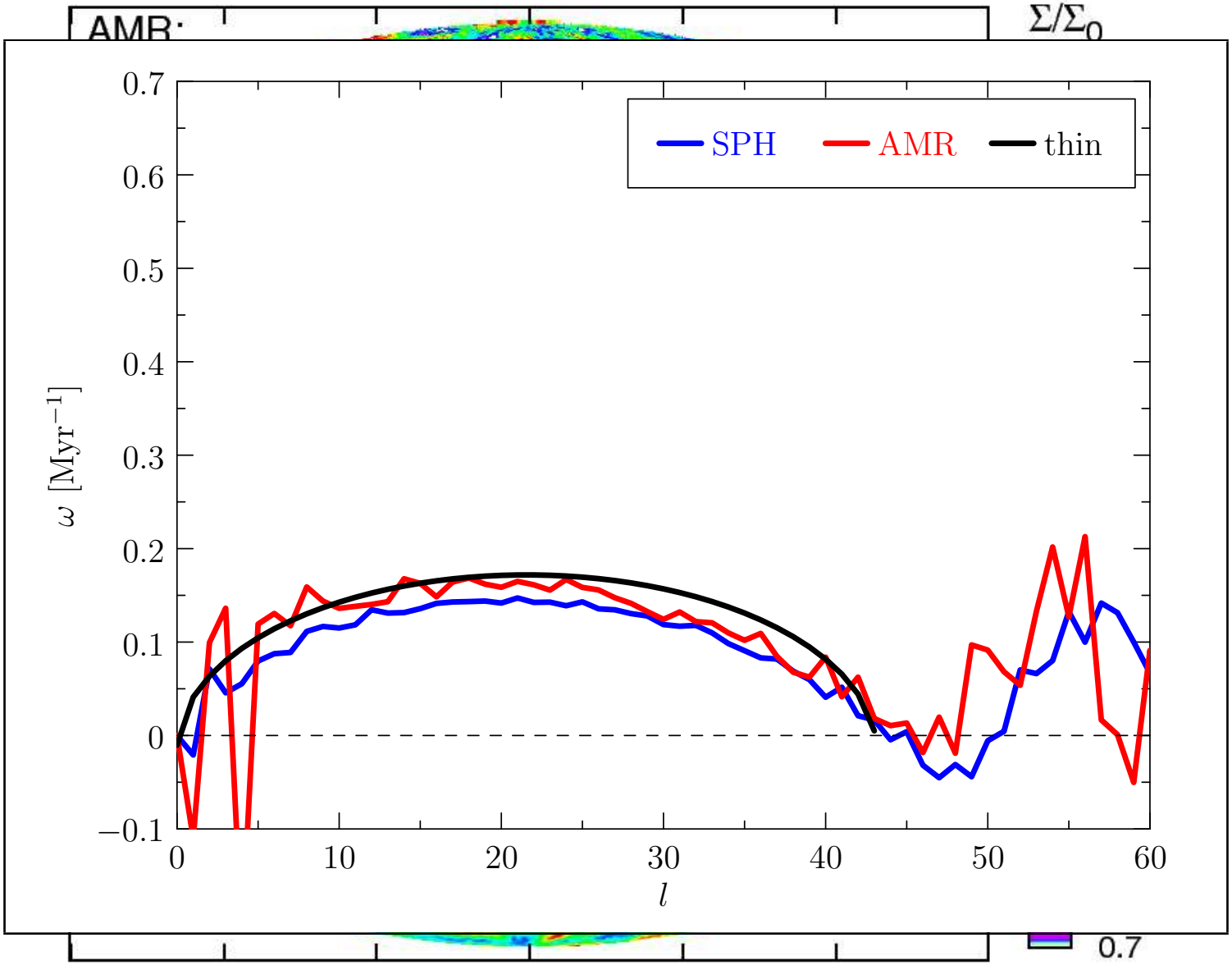

Dispersion relation depends on $P_{\rm ext}$ (and hence on the shell thickness)

$P_{\rm ext} = 10^{-17}$ $P_{\rm ext} = 10^{-13}$ $P_{\rm ext} = 5 \times 10^{-13}$dyne cm^{-2}

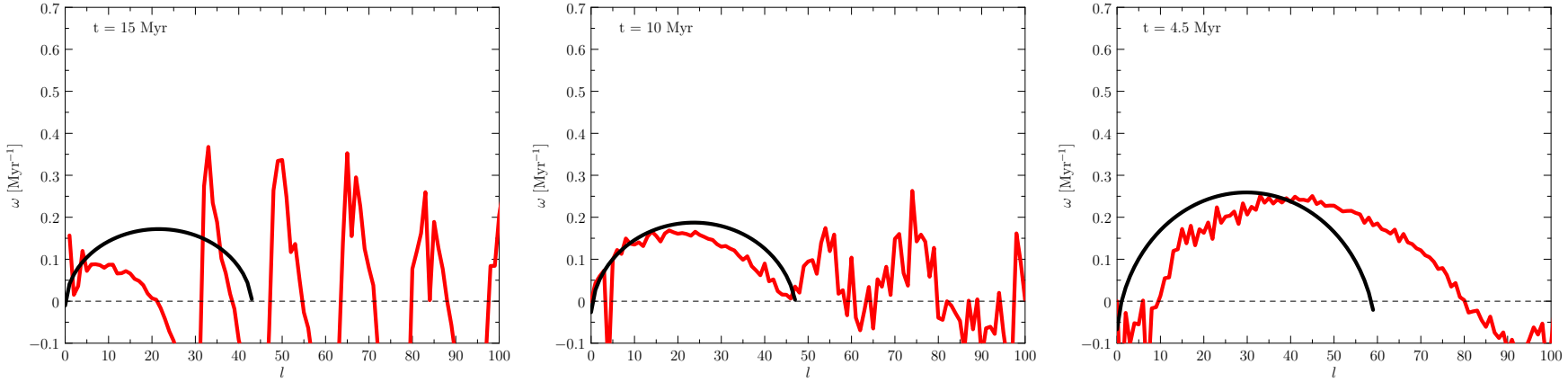

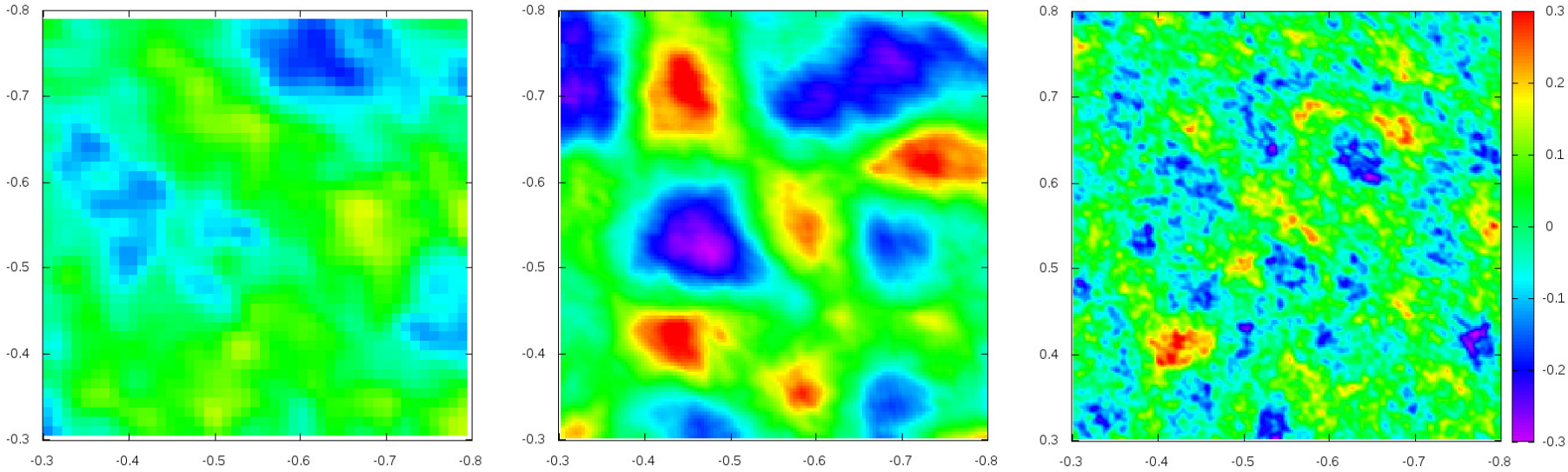

Dependence of fragment growth rate on $P_{\rm ext}$

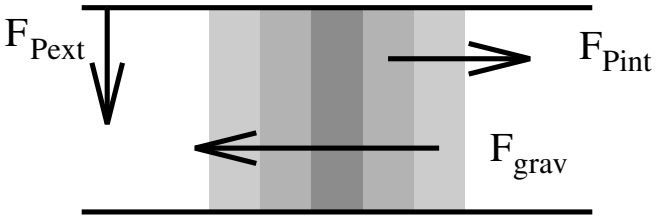

thin shell approx.

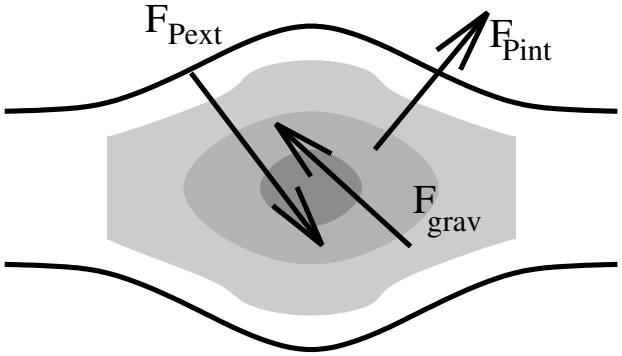

fragments in simulations

- the shell thickness varies across fragments
- external pres. force is not perpendicular to the shell surface

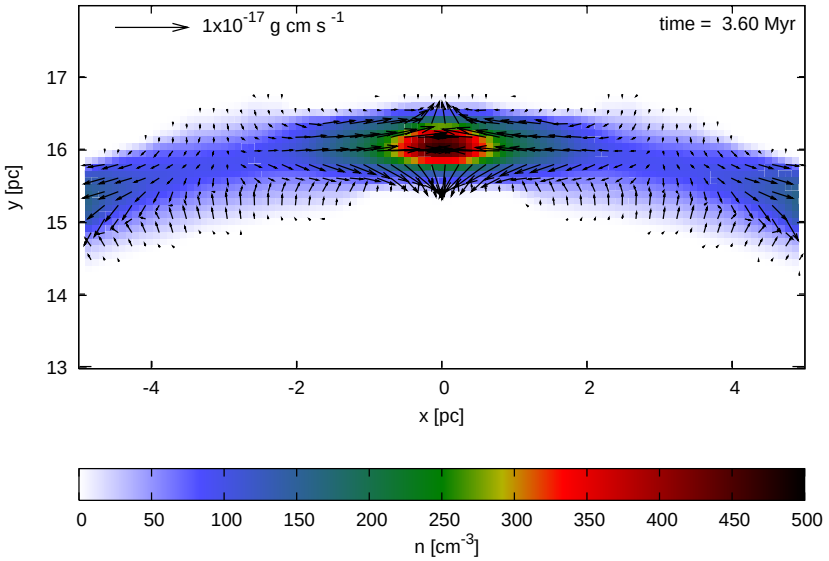

Uniform Oblate Spheroid

(Boyd & Whitworth, 2005)

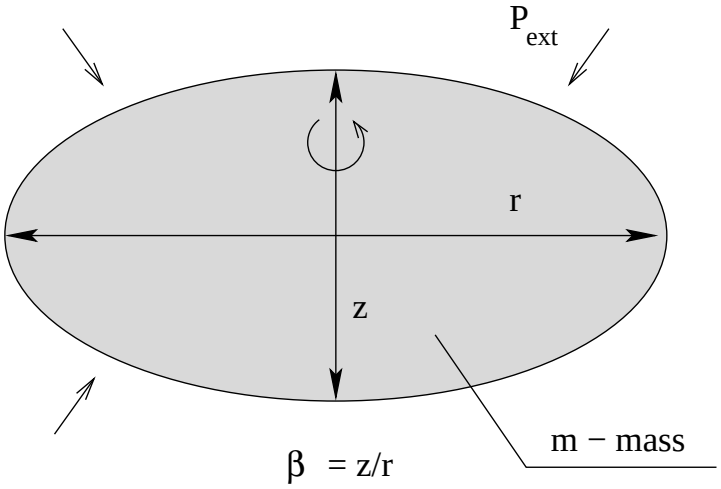

Kinetic, gravitational and compressional energy:

$$\mathcal{K} = \frac{m}{10}\left(2\dot{r}^2 + \dot{z}^2\right)$$

$$\mathcal{G} = -\frac{3\,G\,m^2}{5}\,\frac{\cos^{-1}(z/r)}{\left(r^2-z^2\right)^{1/2}}$$

$$\frac{d\mathcal{B}}{dV} = P_{\rm ext} - P_{\rm int} = P_{\rm ext} - \frac{m\,c_s^2}{V}$$

- energy conservation: $\mathcal{E} = \mathcal{K} + \mathcal{G} + \mathcal{B}$
- differentiate with resp. to time:

$$\left\{\frac{2\,m\,\ddot{r}}{5} + \frac{d\mathcal{G}}{dr} + \frac{d\mathcal{B}}{dr}\right\}\dot{r} + \left\{\frac{m\,\ddot{z}}{5} + \frac{d\mathcal{G}}{dz} + \frac{d\mathcal{B}}{dz}\right\}\dot{z} = 0\,.$$

- $\dot{r}$ and $\dot{z}$ independent:

$$\ddot{r} = -\frac{3Gm}{2r^2}\left[\frac{\cos^{-1}\beta}{(1-\beta^2)^{3/2}} - \frac{\beta}{1-\beta^2}\right] - \frac{20\pi P_{\rm ext} r z}{3m} + \frac{5c_s^2}{r}$$

UOS vs. thin shell

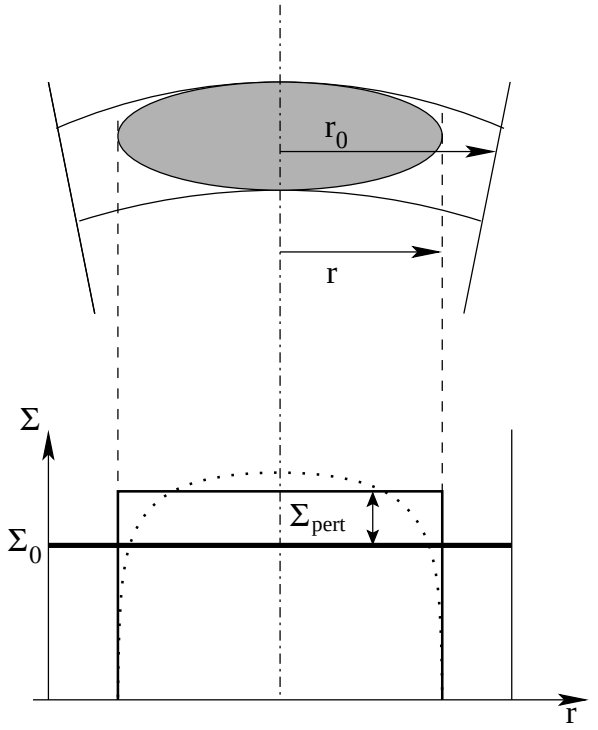

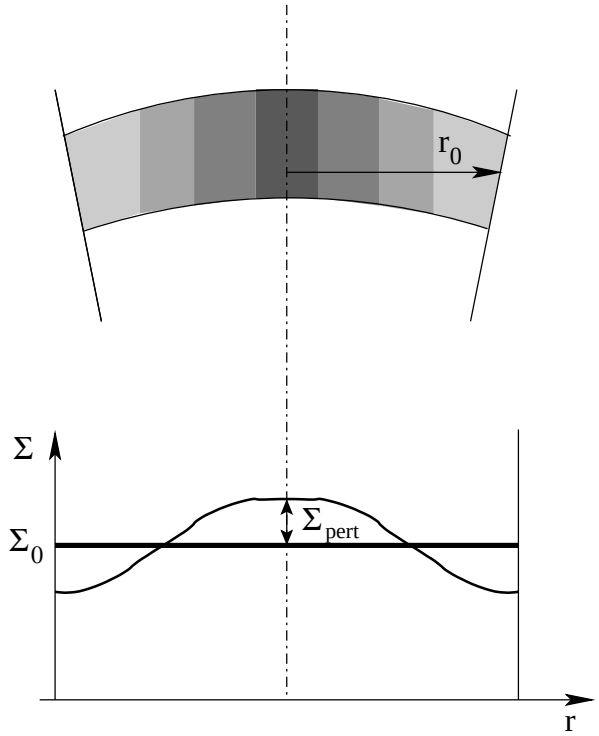

- z given by hydrostatic equilibrium
- non-linear eqs. of motion
- homogeneous ellipsoid

- no vertical structure (inf. thin shell)
- linearized hydrodyn. eqs.
- sinusoidal perturbations

Dispersion relation of the thick shell

$$\omega_\epsilon = -\underbrace{\frac{V}{2R\epsilon}}_{\text{stretching}} + \left\{ \underbrace{\frac{V^2}{4R^2\epsilon^2}}_{\text{stretching}} + \underbrace{\frac{3G\Sigma_0 l}{4R\epsilon}\left[\frac{\cos^{-1}\beta}{(1-\beta^2)^{3/2}} - \frac{\beta}{1-\beta^2}\right]}_{\text{gravity}} \right.$$

$$\left. + \underbrace{\frac{1 - P_{\text{ext}} c_s^2 l^2}{3\pi^2 R^2 \epsilon (2P_{\text{ext}} + \pi G \Sigma_0^2)}}_{\text{external pres.}} \underbrace{- \frac{5 c_s^2 l^2}{2\pi^2 R^2 \epsilon}}_{\text{internal pres.}} \right\}^{1/2} .$$

Conf. to thin shell:

$$\omega_{\text{thin}} = -\underbrace{\frac{3V}{2R}}_{\text{stretching}} + \left(\underbrace{\frac{V^2}{4R^2}}_{\text{stretching}} + \underbrace{\frac{2\pi G \Sigma_0 l}{R}}_{\text{gravity}} \underbrace{- \frac{c_s^2 l^2}{R^2}}_{\text{internal pres.}} \right)^{1/2}$$

- geometry factor at gravity term
- external pressure term
- dependence on ϵ - shrink fraction

Pressure assisted gravitational instability

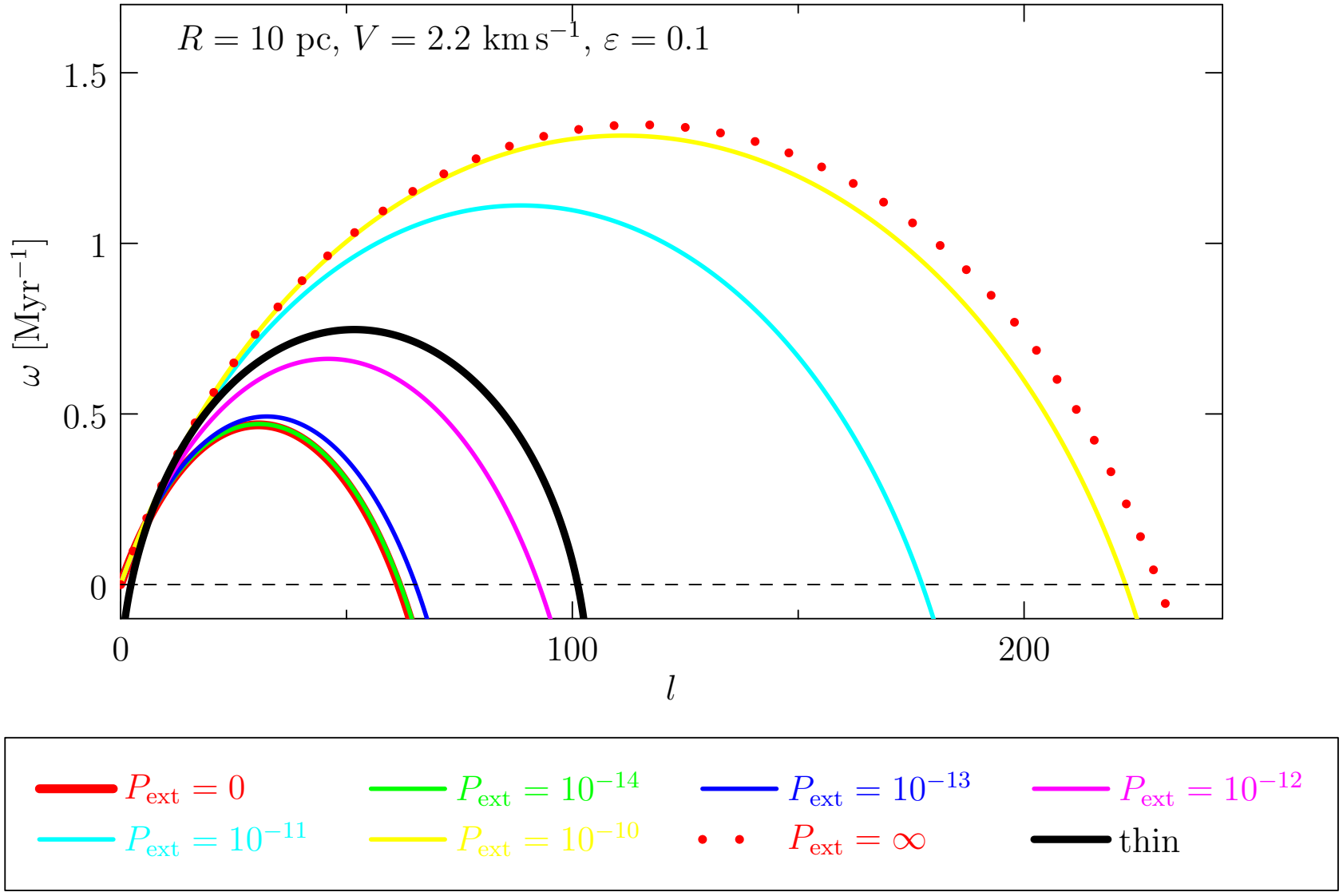

Critical external pressure: $\omega_\epsilon \sim \omega_{\rm thin}$

- $\omega_\epsilon \sim \omega_{\rm thin}$ for $P_{\rm ext,crit}$ for which $\frac{dz}{d\Sigma} = 0$
  (the shell thickness does not depend on the surface density)

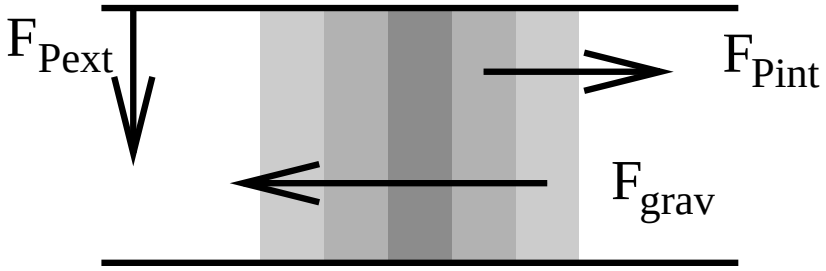

thin shell approx.

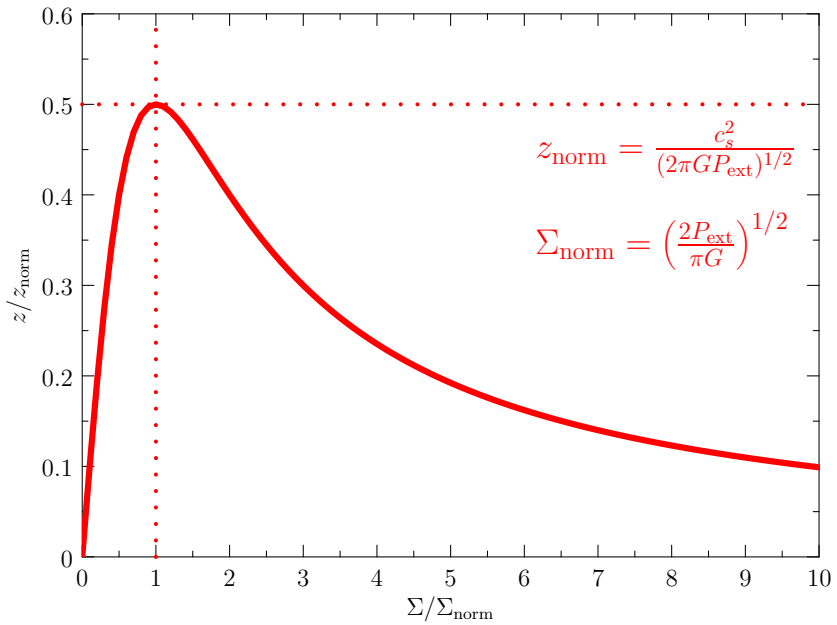

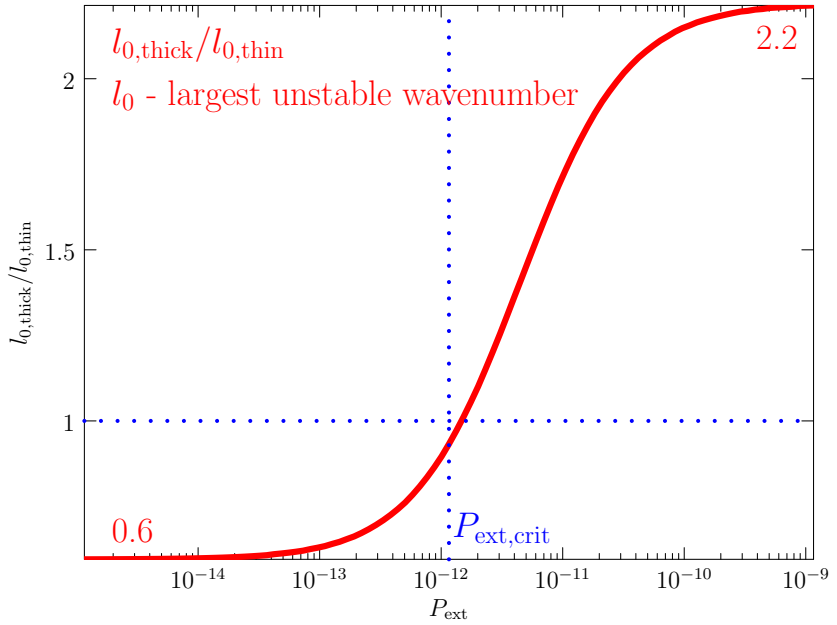

PAGI vs. simulations

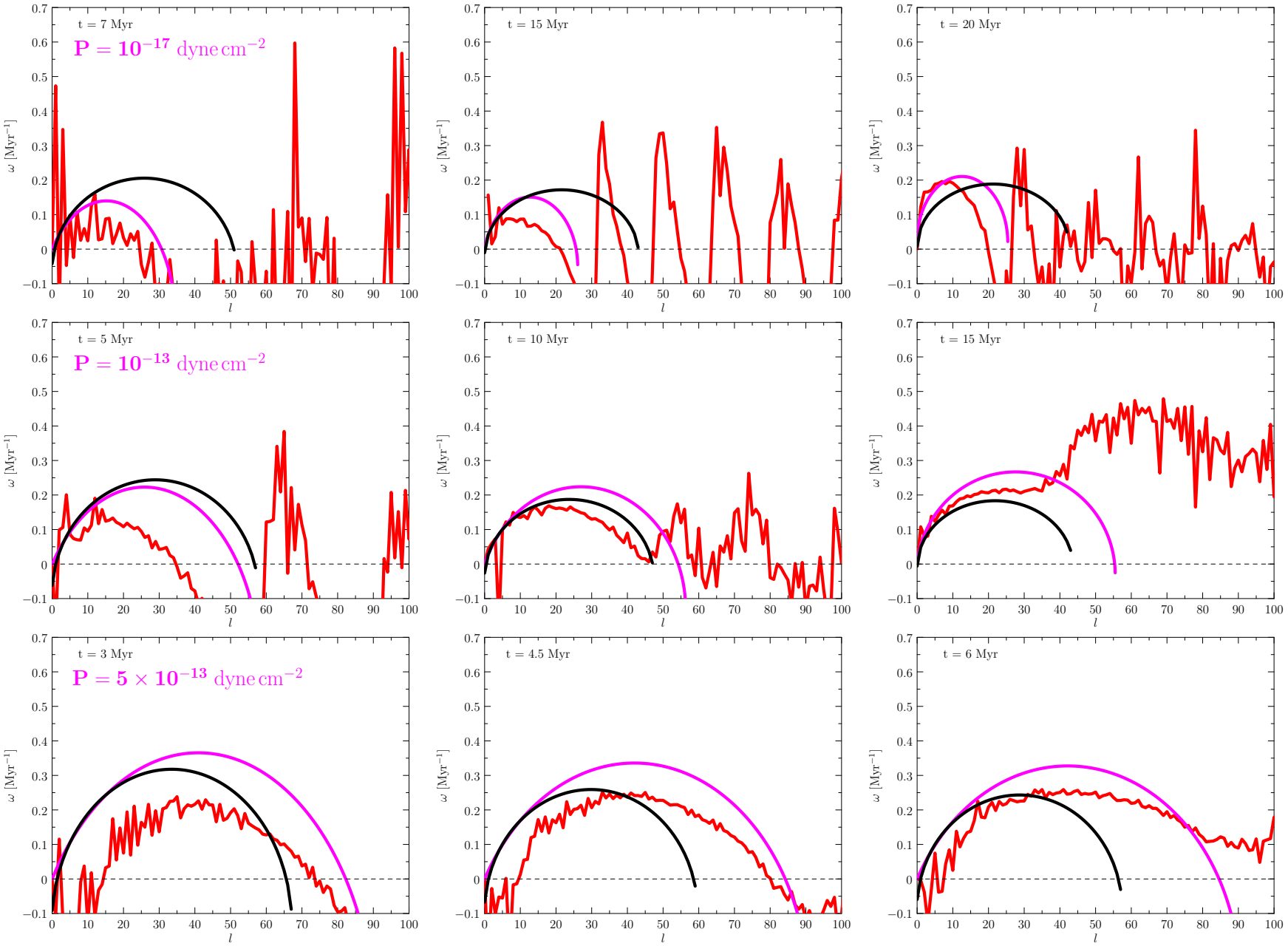

Mass spectrum from Fragmentation Integral

$$\frac{dN}{dm} \sim I_{\rm f}(l,t) \times m^{-2}$$

where $I_{\rm f}(l,t) = \int \omega(l,t')dt'$ is **the fragmentation integral**

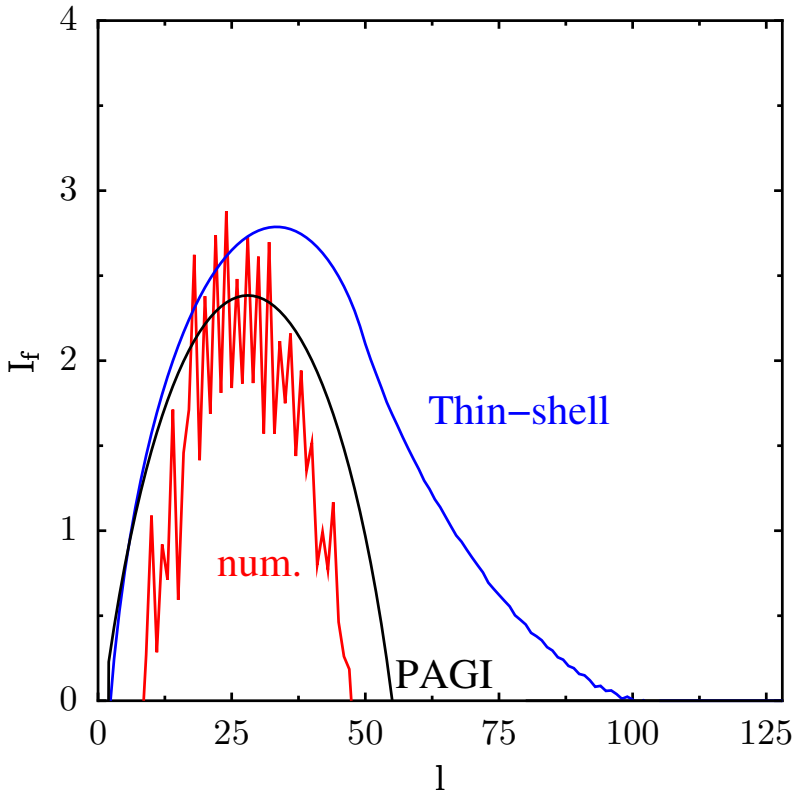

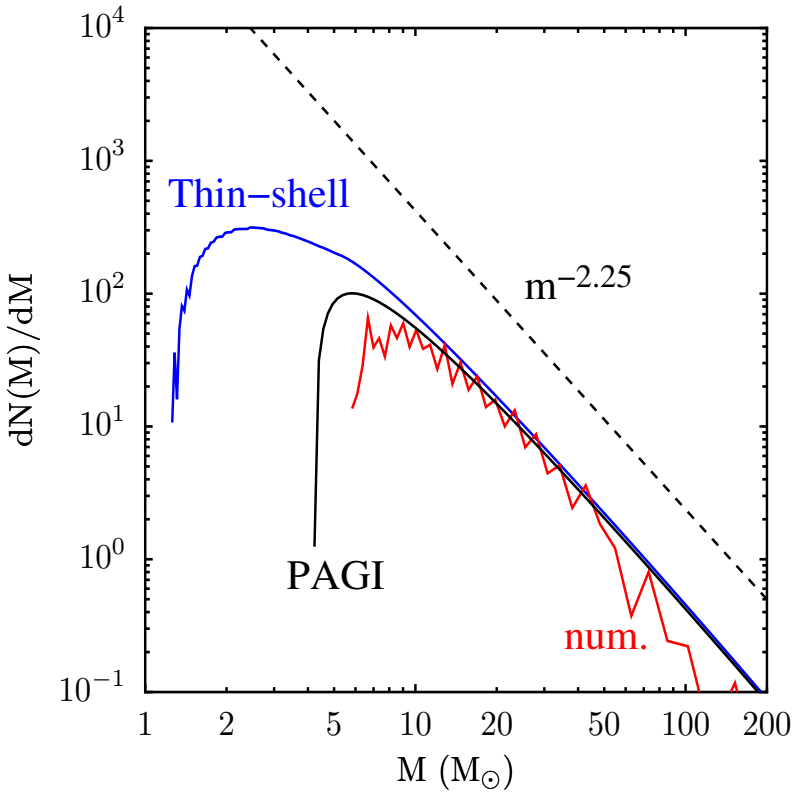

Mass spectrum of clumps

- clumps identified by algorithm by Smith et al (2009) (similar to CLUMPFIND, but uses grav. potential instead of density)
- initially agrees well with mass spectrum obtain from the fragmentation integral
- later, it becomes more and more top-heavy

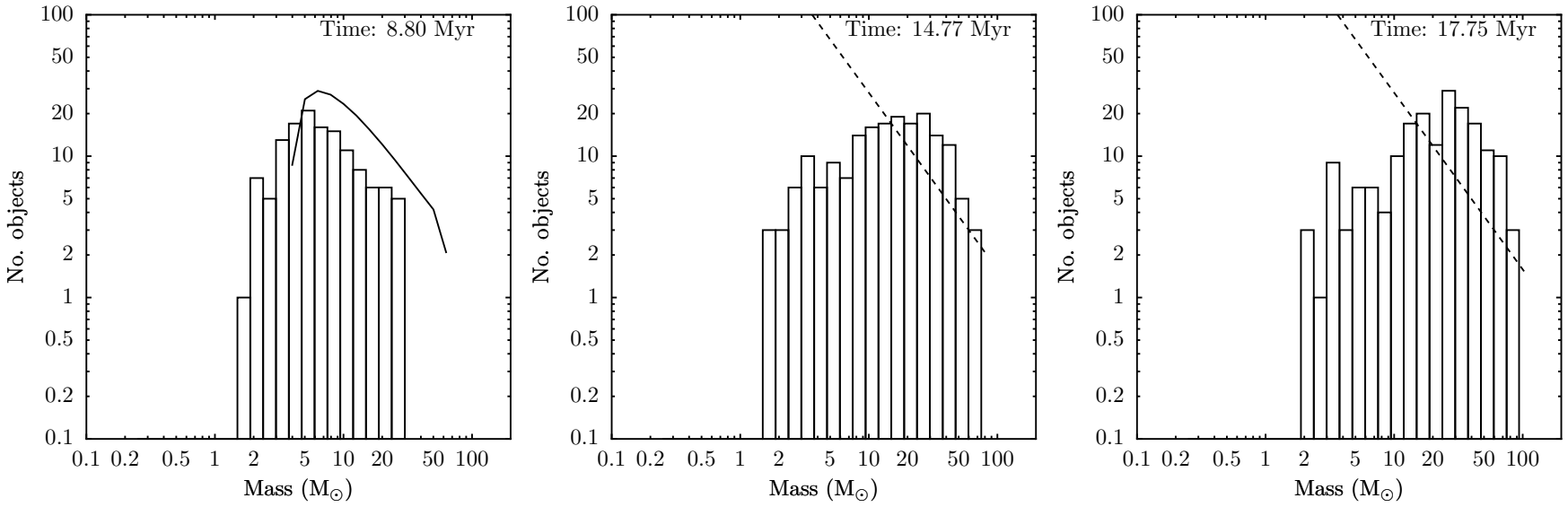

Mass spectrum of sink particles

- sink particles created if gravitationally collapsing gas reaches resolution limits
- sink mass function is even more top-heavy
- peaks at $M \sim 80$ $\mathrm{M}_\odot$ which corresponds to $l = 25$, most unstable wavenumber at the time shell reaches maximum radius

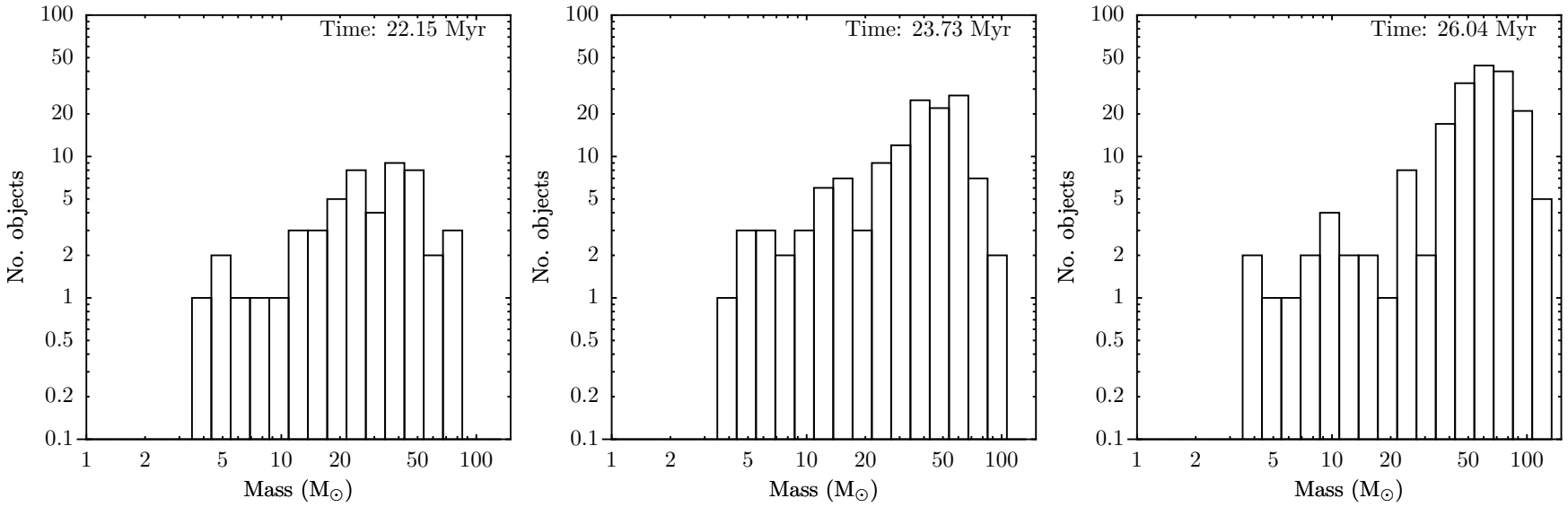

Oligarchic accretion

- period of high sink formation rate
- "oligarchs" from this period consume most of shell mass

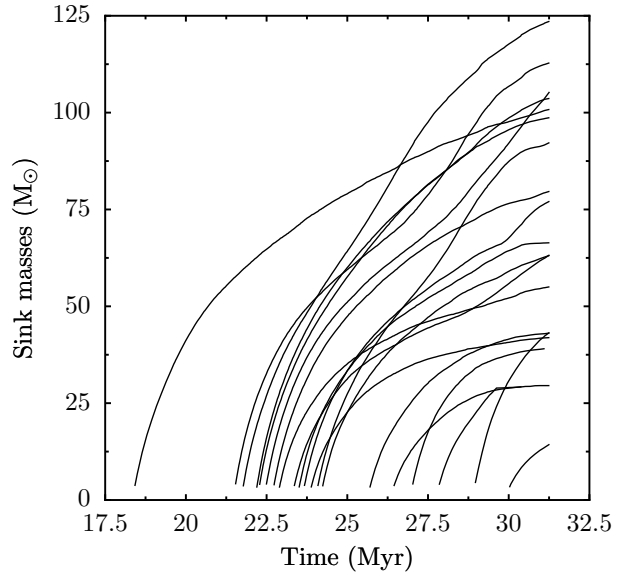

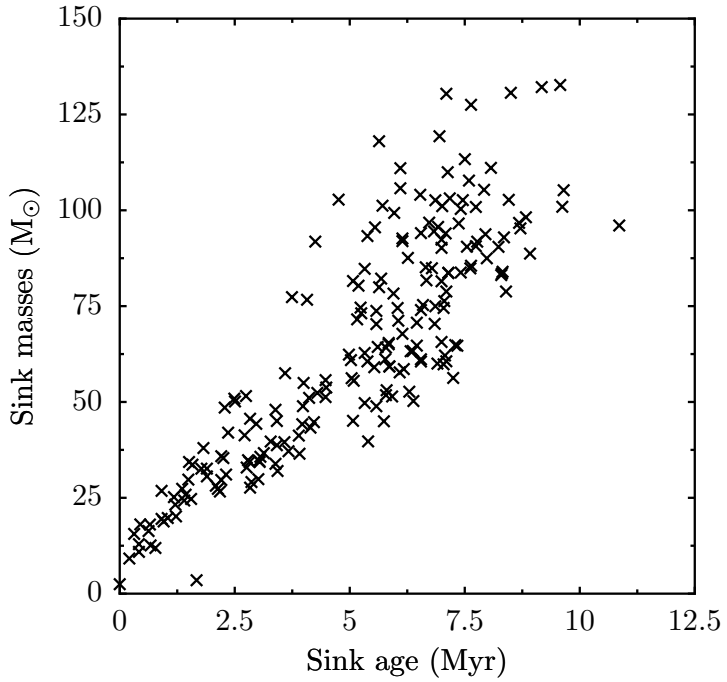

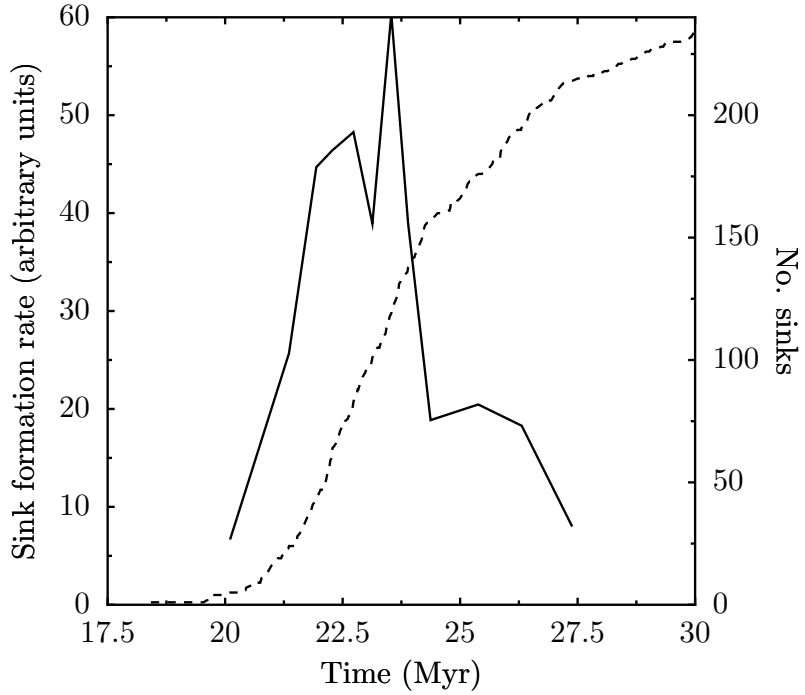

Discussion

- PAGI gives systematically larger range of unstable wavelengths than simulations (?approximation of the UOS evolution by constant acceleration)
- ω only amplifies initial spectrum (given by the turbulence, . . .)
- we assume shell confined by thermal pressure from both sides, but instability can be different if the ram pressure confines the shell from outside (accreting shell)
- Vishniac and RT instabilities may have an impact
- Oligarchic accretion and the resulting top-heavy CMF appear because the gas reservoir to form new cores is depleted (shell does not accrete); Klessen & Burkert (2000) observe similar process in evolution of turbulent protocluster if SFE is high

Carina Flare Supershell observarion

- PAGI predicts deficit of low mass fragments in low pres environments (and vice versa)
- Oligarchic accretion predicts top-heavy CMF for non-accreting shells
- we plan to use the APEX telescope (got 36 hours) to determine CMF of the Carina Flare supershell (extends ~ 450 pc above the galactic plane)

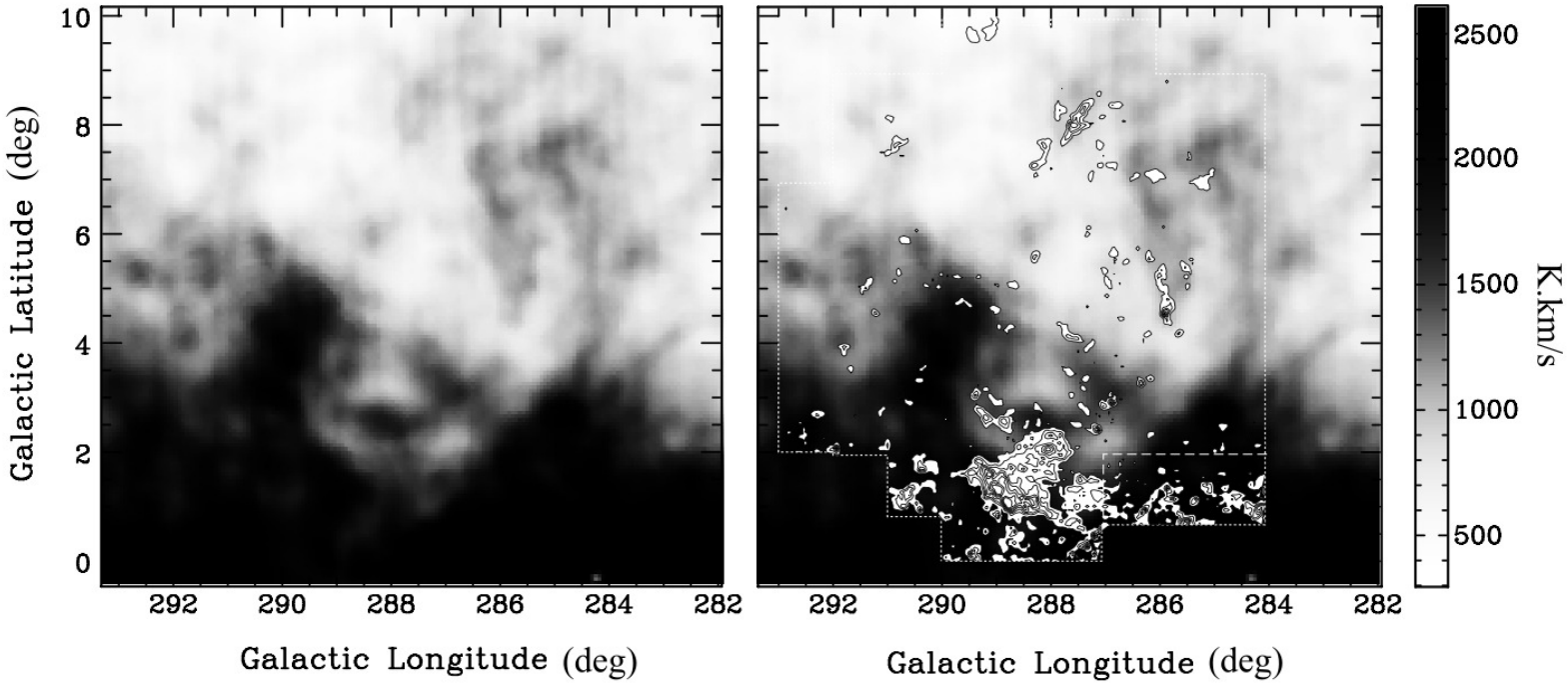

Conclusions

- excellent agreement between AMR and SPH, but disagreement with the thin shell approximation
- new instability (PAGI) and dispersion relation (fragment growth rate) for the thick shell embedded in the medium with non-zero pressure
- the PAGI dispersion relation depends on the external pressure, predicts range of unstable wavenumbers different than the one given by the thin shell approximation by factor of 0.6 and 2.2 for $P_{\rm ext} = 0$ and ∞, respectively
- the PAGI dispersion relation is similar to the thin shell one for the pressure for which the shell thickness locally does not depend on its surface density (maximum shell thickness)
- early stage: mass spectrum of clumps agrees well with analytical estimates (PAGI)
- later stage: oligarchic accreation leads to the top-heavy CMF

References

Dale, J. E., Wünsch, R., Whitworth, A., Palouš, J., 2009, MNRAS, 398, 1537

Wünsch, R., Dale, J. E., Palouš, J., Whitworth, A., 2010, MNRAS, 407, 1963

Dale, J. E., Wünsch, R., Smith, R. J., Whitworth, A., Palouš, J., 2010, MNRAS, in press

Boyd & Whitworth, 2005, A&A, 430, 1059

Churchwell, E., etal, 2006, ApJ, 649, 759

Deharveng, L., Lefloch, B.; Zavagno, A.; Caplan, J.; Whitworth, A. P.; Nadeau, D.; Martín, S.2003, A&A, 408, L25

Ehlerová, S., Palouš, J., 2005, A&A, 437, 101

Elmegreen, B. G., Lada, C. J., 1977, ApJ, 214, 725

Elmegreen, B. E., 1994, ApJ, 427, 384

Garcia-Segura, G., Franco, J., 1996, ApJ, 496, 171

Klessen, R., Burkert, A., 2000, ApJS, 128, 287

Parker, E. N., 1966, ApJ, 145, 811

Sidorin, V. 2008, Master thesis, Charles University

Smith, R. J., Clark, P. C., Bonnell, I. A., 2009, MNRAS, 396, 830

Vishniac, E. T., 1983, ApJ, 274, 152

Wardle, M. 1990, MNRAS, 246, 98